# Robust Propagation of Two-Color Soliton Clusters Supported by Competing Nonlinearities

Yaroslav V. Kartashov,[1,2] Lucian-Cornel Crasovan,[1,3] Dumitru Mihalache,[1,3] and Lluis Torner[1]

[1]*Institute of Photonic Sciences and Department of Signal Theory and Communications, Universitat Politecnica de Catalunya, 08034, Barcelona, Spain*
[2]*Physics Department, M.V. Lomonosov Moscow State University, 119899, Moscow, Russia*
[3]*Department of Theoretical Physics, Institute of Atomic Physics, Bucharest, Romania*
(Received 28 June 2002; published 19 December 2002)

We reveal numerically the remarkably robust propagation of quasistationary two-color soliton clusters in media with competing quadratic and cubic nonlinearities. We predict that such clusters carrying nonzero angular momentum can propagate over any practically feasible crystal length before they decay, even in the presence of input random perturbations.

Solitons play a crucial role in many branches of nonlinear science. They form from the proper balance between linear spreading effects and adequate nonlinear effects in a variety of physical systems, including hydrodynamics (shallow- and deep-water waves), plasma physics (charge-density waves), atomic physics (matter-wave solitons), and optics (e.g., fiber, cavity, quadratic, photorefractive, incoherent, and discrete solitons) [1–7]. Optical solitons are self-trapped light beams or pulses that are supported by a balance between diffraction and/or dispersion and various types of nonlinearities [2]. Several types of optical solitons have been identified and observed experimentally during the last two decades, and main properties of the corresponding individual solitons are well understood now [3]. However, one of the main challenging open frontiers of the field is the elucidation of experimentally observable, quasistationary complex soliton structures, or clusters, which can be viewed as "soliton molecules." Such a concept—hence the results we report here—might prove useful in other fields besides optics, such as the Skyrme model of classical field theory [4] and to the formation of complex soliton structures in atom optics and in trapped Bose-Einstein condensates [5–7].

The concept of optical soliton cluster was introduced as a generalization of necklace-ring beams studied in Kerr-like and photorefractive media [8,9]. Soliton clusters in non-Hamiltonian systems have been considered too [10]. However, the formation of soliton clusters in single-pass geometries leads to expanding or, at best, metastable structures. In the numerical simulations, metastable clusters can propagate steadily over significant distances under ideal, unperturbed conditions but the presence of small perturbations leads always to the cluster destruction [9]. In the case of multicolor solitons [11], the expanding clusters can be generated using induced breakup techniques, and thus have been observed experimentally recently in a quadratic nonlinear medium [12]. Expanding clusters also generate spontaneously by the azimuthal modulational instability of the corresponding

ringlike bright vortex solitary-wave solutions [13,14], a feature that was also observed experimentally [15]. However, recently it was shown that a weak self-defocusing cubic nonlinearity can have a strong stabilizing effect on ringlike soliton structures in media with the dominant quadratic nonlinearity [16], and as a result relatively broad optical vortices with topological charge $M = 1$ were found to be stable. The question is whether quasistable clusters might also exist in media with competing nonlinearities. In this Letter, we show that such is the case. We investigate soliton clusters propagating in bulk media with competing quadratic and cubic nonlinearities, and reveal the existence of "soliton molecules" that exhibit quasistable propagation, even in the presence of random deviations of the ideal input conditions.

Under appropriate conditions, the propagation of light beams in media with competing quadratic and cubic nonlinearities under conditions for noncritical phase-matching second-harmonic generation can be described by the following reduced equations [16–18]:

$$i\frac{\partial q_1}{\partial \xi} = \frac{d_1}{2}\left(\frac{\partial^2 q_1}{\partial \eta^2} + \frac{\partial^2 q_1}{\partial \zeta^2}\right) - q_1^* q_2 \exp(-i\beta\xi)$$
$$+ \sigma q_1(|q_1|^2 + 2|q_2|^2),$$
$$i\frac{\partial q_2}{\partial \xi} = \frac{d_2}{2}\left(\frac{\partial^2 q_2}{\partial \eta^2} + \frac{\partial^2 q_2}{\partial \zeta^2}\right) - q_1^2 \exp(i\beta\xi)$$
$$+ 2\sigma q_2(2|q_1|^2 + |q_2|^2). \qquad (1)$$

Here $q_1 = (2k_1/k_2)^{1/2}(2\pi\omega_0^2\chi^{(2)}r_0^2/c^2)A_1$, $q_2 = (2\pi\omega_0^2\chi^{(2)}r_0^2/c^2)A_2$ are the amplitudes of the fundamental frequency ($\omega = \omega_0$) and second-harmonic ($\omega = 2\omega_0$) waves, $k_1 = k(\omega_0)$ and $k_2 = k(2\omega_0)$ are the wave numbers, $k_2 \approx 2k_1$, $A_{1,2}(\eta, \zeta, \xi)$ are the slowly varying envelopes, $r_0$ is the transverse scale of input beams, $\eta = x/r_0$ and $\zeta = y/r_0$ are the normalized transverse coordinates, $\xi = z/k_1 r_0^2$ is the normalized propagation distance, $d_1 = -1$, $d_2 = -k_1/k_2 \approx -1/2$, $\beta = (2k_1 - k_2)k_1 r_0^2$ is the phase mismatch, $\sigma = (3\chi^{(3)}/8\pi)(c/\omega_0\chi^{(2)}r_0)^2$, and $\chi^{(2)}$ and $\chi^{(3)}$ are appropriate nonlinear susceptibilities. In the numerical simulations we used $\sigma = 0.2$. Notice that

Eqs. (1) correspond to the simplest model of light propagation in media with competing nonlinearities (e.g., it assumes a noncritical, type I, *oo* or *ee* wave interaction). In practice, the strength of each of the possible cross-phase modulations depends critically on the crystalline symmetry of the particular material employed through

the polarizations of the fields involved, hence the actual value of the relevant elements of the nonlinear susceptibility tensor [18]. However, Eqs. (1) are expected to capture the essentials of the process. They constitute a Hamiltonian system that possesses several conserved quantities. Among them are the Hamiltonian $H$ and the total energy flow $U$:

$$H = -\frac{1}{2} \int_{-\infty}^{\infty} d\eta \int_{-\infty}^{\infty} [d_1|\nabla q_1|^2 + (d_2/2)|\nabla q_2|^2$$
$$+ q_1^{*2} q_2 \exp(-i\beta\xi) + q_1^2 q_2^* \exp(i\beta\xi) - \beta|q_2|^2 - \sigma(|q_1|^4 + 4|q_1|^2|q_2|^2 + |q_2|^4)]d\zeta, \quad (2)$$

$$U = \int_{-\infty}^{\infty} d\eta \int_{-\infty}^{\infty} d\zeta(|q_1|^2 + |q_2|^2).$$

Here $\nabla = \mathbf{e}_\eta(\partial/\partial\eta) + \mathbf{e}_\zeta(\partial/\partial\zeta)$; $\mathbf{e}_\eta$ and $\mathbf{e}_\zeta$ are the unit vectors in the directions of $\eta$ and $\zeta$, respectively. We construct soliton clusters as a superposition of the lowest-order bell-shaped solitons. The profiles of such solitons can be found from the system of Eqs. (1) with the aid of the substitution $q_{1,2}(\eta, \zeta, \xi) = q_{1,2}(r, \varphi, \xi) = w_{1,2}(r)\exp(ib_{1,2}\xi + im_{1,2}\varphi)$, where $w_{1,2}(r)$ are real functions of coordinate $r = (\eta^2 + \zeta^2)^{1/2}$, $\varphi$ is the azimuthal angle, $b_{1,2}$ are the propagation constants ($b_2 = \beta + 2b_1$), and $m_{1,2} = 0$. Figure 1 shows Hamiltonian-energy flow diagrams and profiles of the lowest-order solitons for three representative values of the phase mismatch $\beta$. Note that even for weak cubic nonlinearity ($\sigma = 0.2$) the solitons in media with competing nonlinearities are much wider than the corresponding solitons in purely quadratic media. Next we concentrate on the case $\beta = 0$. The construction of soliton clusters from the lowest-order solitons enables one to avoid the radiation of the nonsolitonic part of the energy in the process of cluster propagation. Hence, we set the initial field distribution in the following way:

$$q_1(\eta, \zeta, \xi = 0) = \sum_{n=1}^{N} \exp(i\psi n)w_1(r_n),$$
$$q_2(\eta, \zeta, \xi = 0) = \sum_{n=1}^{N} \exp(2i\psi n)w_2(r_n), \quad (3)$$

where $N$ is the number of solitons forming the cluster, $\psi = 2\pi M/N$ is the phase difference between neighboring solitons, $M = 0, 1, 2, \ldots$, is the topological charge of the cluster, the functions $w_{1,2}$ describe profiles of identical solitons forming the cluster, $r_n = \{[\eta - R_0\cos(2\pi n/N)]^2 + [\zeta - R_0\sin(2\pi n/N)]^2\}^{1/2}$, where $n = 1, 2, \ldots, N$, and $R_0$ is the input radius of the cluster.

The evolution of the soliton cluster is dictated by the interaction forces acting between neighboring solitons and depending on the value of the energy flow, initial cluster radius, relative phase between the solitons forming the cluster and material parameters. The simplest way to obtain a rich variety of propagation regimes is to modify the cluster charge $M$, keeping fixed the number of solitons $N$. It is convenient to classify all possible regimes of propagation of the soliton clusters by looking at the dependence of the cluster mean (or integral) radius

$$R = (1/U) \int_{-\infty}^{\infty} d\eta \int_{-\infty}^{\infty} d\zeta(\eta^2 + \zeta^2)^{1/2}(|q_1|^2 + |q_2|^2)$$

on the propagation distance $\xi$ (here $U$ is the total cluster energy flow).

In the case when $M = nN$ ($n = 0, 1, 2, \ldots$) the cluster has zero angular momentum. The solitons attract each other and the cluster fuses in the process of propagation into a single lowest-order soliton; the damped oscillations of the cluster radius are clearly seen during evolution [Fig. 2(a)]. We show only the intensity distributions for the fundamental wave since the second-harmonic wave exhibits similar features. The cluster has zero angular momentum also for even $N$ and $M = (2n + 1)N/2$ ($n = 0, 1, 2, \ldots$). Such clusters expand in the process of propagation since the interaction potential between different solitons is now repulsive [Fig. 2(b)]. When $(n + 1/4)N \leq M \leq (n + 3/4)N$ and $M \neq (2n + 1)N/2$ ($n = 0, 1, 2, \ldots$), the cluster has a nonzero orbital angular momentum.
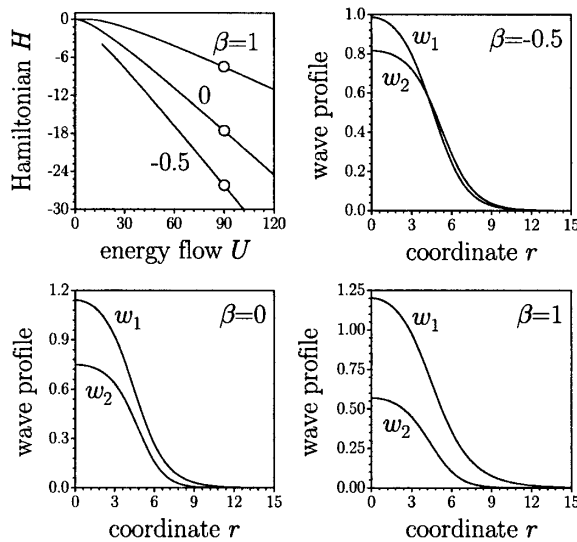


FIG. 1. Hamiltonian-energy flow diagram and typical soliton profiles for various phase mismatches. Shown profiles correspond to marked points at the Hamiltonian-energy flow diagram. Parameter $\sigma = 0.2$.
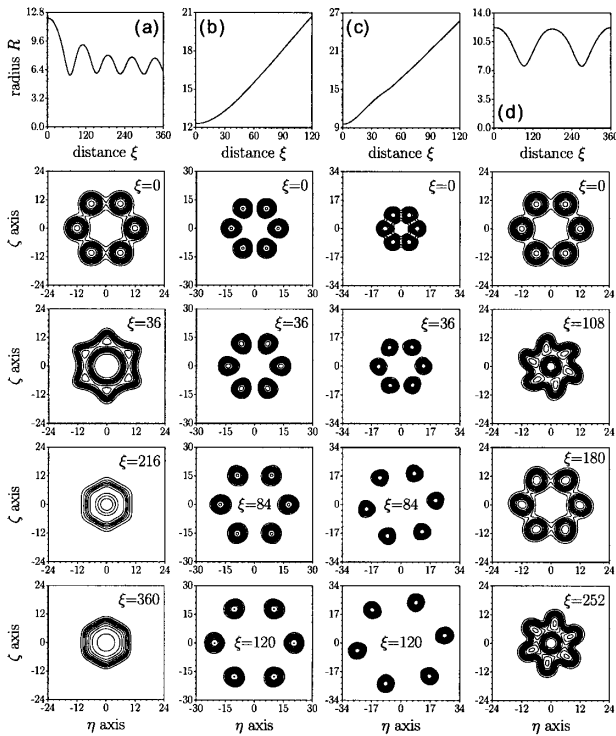
FIG. 2. Different propagation regimes of multicolor soliton clusters with $N = 6$. The first row shows the evolution of the cluster mean radius upon propagation. The contour plots show the intensity distribution in the fundamental wave at various propagation distances. (a) $M = 0$, $R_0 = 12$; (b) $M = 3$, $R_0 = 12$; (c) $M = 2$, $R_0 = 9$; (d) $M = 1$, $R_0 = 12$. All clusters are constructed from solitons with energy flow $U = 90$, at $\beta = 0$ and $\sigma = 0.2$.

The propagation of such clusters is accompanied by their simultaneous expansion and rotation [Fig. 2(c)]. When $(n - 1/4)N \leq M \leq (n + 1/4)N$ and $M \neq nN$ ($n = 0, 1, 2, \dots$) neighboring solitons in cluster attract each other; however, the nonzero angular momentum of the whole structure prevents constituent solitons from fusion. Thus for relatively large input radius $R_0$ the cluster periodically shrinks to its minimal radius and expands to its initial size. This process is accompanied by rotation of the cluster [Fig. 2(d)]. Conversely, the cluster with small enough $R_0$ expands at the initial stage of propagation and then restores its initial profile. Such behavior of the clusters with $(n - 1/4)N \leq M \leq (n + 1/4)N$, $M \neq nN$, suggests the possibility of formation of quasistationary clusters that rotate upon propagation but conserve their radiuses. To gain further insight, we implemented an approximate interaction-potential approach [9,19] that predicts the existence of energetically favorable cluster states with balanced attraction repulsion (Fig. 3). The model was found to give valuable information, but the predicted radius for balanced interaction was often found to depart from the actual radius of quasistable propagation, a fact attributed to the large overlap between the solitons which turns
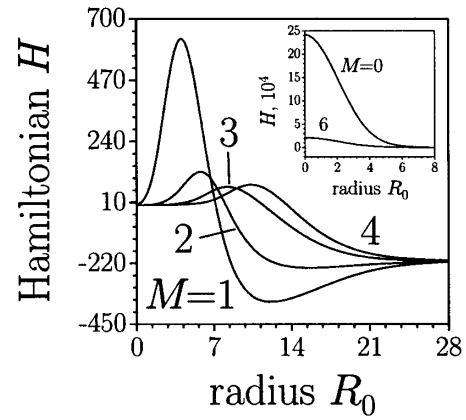
FIG. 3. Dependencies of the Hamiltonian of the cluster on initial cluster radius for various charges $M$ at $N = 12$. Cluster is constructed from solitons with energy flow $U = 90$, at $\beta = 0$ and $\sigma = 0.2$.

the effective-potential approach correspondingly less accurately.

Typical examples of actual quasistationary clusters are shown in Figs. 4(a) and 4(b). Note that the input radii $R_0$ of such clusters are relatively small, so that the neighboring solitons overlap considerably. The evolution of the
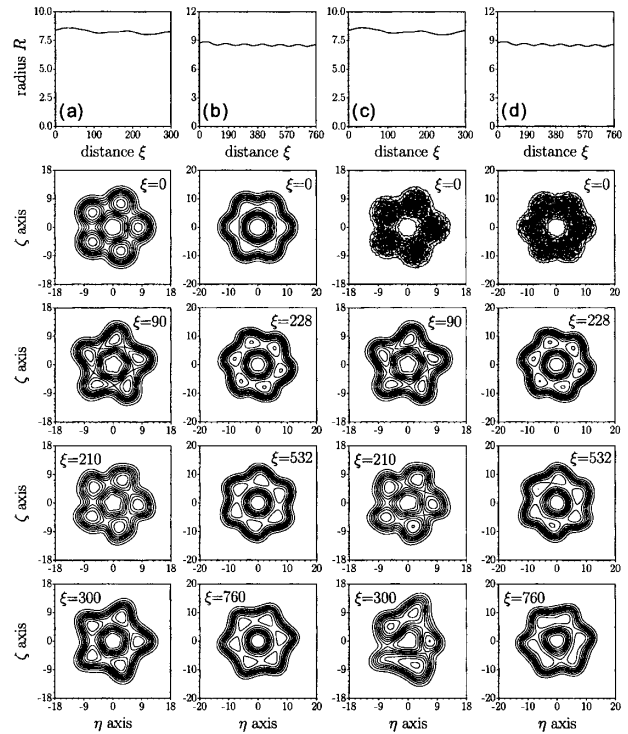


FIG. 4. Propagation dynamics of quasistationary clusters. The first row shows the evolution of the cluster mean radius upon propagation. (a) $N = 5$, $M = 1$, $R_0 = 8$; (b) $N = 6$, $M = 1$, $R_0 = 8.45$; the columns (c) and (d) show the propagation of the same clusters as in the columns (a) and (b) but in the presence of a Gaussian noise with $\sigma_{1,2}^2 = 0.02$. The other parameters are as in Fig. 2.

quasistationary cluster depends on the total energy flow of the whole structure. If the cluster energy flow is close to that corresponding to the stationary ringlike vortex soliton, the reshaping of the whole structure is minimal, whereas if the cluster energy flow greatly exceeds that necessary for the formation of the ringlike vortex, the reshaping leads usually to the formation of additional rings inside the initial cluster. One finds that for a fixed charge $M$ there exists an optimal number of solitons $N$ for which the reshaping upon propagation is minimal.

The important result put forward in this Letter is the robustness on propagation of the soliton clusters studied, in contrast to previously known soliton clusters in both quadratic and in cubic nonlinear media [8,9,14], which are all affected by self-demolition azimuthal modulation instabilities. To show this key point we added random noise to the initial clusters by multiplying (3) by $[1 + \rho_{1,2}(r, \varphi)]$, where $\rho_{1,2}(r, \varphi)$ is the Gaussian random function with $\langle \rho_{1,2} \rangle = 0$ and $\langle \rho_{1,2}^2 \rangle = \sigma_{1,2}^2$. Typical evolution of the perturbed clusters is shown in Figs. 4(c) and 4(d). One observes that even with the random deviations of the input (clearly visible on the plot), the clusters keep their structure for several hundreds of diffraction lengths, 2 orders of magnitude larger than the experimentally feasible crystal lengths. Under identical conditions, a cluster in a pure quadratic medium is destroyed in a few mm. The robustness of the clusters increases with the number of solitons, a result that seems to be consistent with the stabilization of vortex solitons with $M = 1$ [16]. However, notice the key physical difference existing between vortex solitons, which feature a continuous wave front, and the clusters studied here, which are built as the discrete superposition of individual solitons, thus featuring discrete phase dislocations between them. Thus, e.g., while stabilized vortex solitons with $M = 2$ were found to exist [16], we found that the corresponding clusters decay much faster than the clusters with $M = 1$. Finally, the simulations show [e.g., Fig. 4(c)] that even the clusters with $M = 1$ eventually self-destroy as a result of the asymmetric interaction and fusion of neighbor solitons. Separate series of simulations, not shown here, revealed that in the presence of competing nonlinearities the interaction between solitons weakened in comparison with soliton interactions in purely quadratic media. We attribute the robustness of the soliton clusters uncovered in this work to such weakened soliton-soliton interaction.

We conclude by noting the potential applicability of the phenomenon uncovered here to analogous physical systems, in which focusing-defocusing, attractive-repulsive nonlinear self-actions compete with each other. We point out that optical competing nonlinearities can occur, e.g., in quadratic nonlinear crystals cut along a suitable axis [20], or in settings where frequency generation is accompanied by optical rectification [21,22]. Competing nonlinearities have also been suggested in atomic-molecular Bose-Einstein condensates [23].

[1] M. J. Ablowitz and P. A. Clarkson, *Solitons, Nonlinear Evolution Equations and Inverse Scattering* (Cambridge University Press, Cambridge, U.K., 1991).

[2] N. N. Akhmediev and A. Ankiewicz, *Solitons* (Chapman-Hall, London, 1997).

[3] M. Segev and G. I. Stegeman, Phys. Today **51**, No. 8, 42 (1998); G. I. Stegeman *et al.*, IEEE J. Sel. Top. Quantum Electron. **6**, 1419 (2000).

[4] R. A. Battye and P. M. Sutcliffe, Phys. Rev. Lett. **86**, 3989 (2001).

[5] K. E. Strecker *et al.*, Nature (London) **417**, 150 (2002); L. Khaykovich *et al.*, Science **296**, 1290 (2002).

[6] J. R. Anglin and W. Ketterle, Nature (London) **416**, 211 (2002).

[7] B. P. Anderson and P. Meystre, Opt. Photonics News **13**, 20 (2002).

[8] M. Soljacic *et al.*, Phys. Rev. Lett. **81**, 4851 (1998); M. Soljacic and M. Segev, Phys. Rev. E **62**, 2810 (2000); Phys. Rev. Lett. **86**, 420 (2001).

[9] A. S. Desyatnikov and Yu. S. Kivshar, Phys. Rev. Lett. **87**, 033901 (2001); **88**, 053901 (2002).

[10] A. G. Vladimirov *et al.*, Phys. Rev. E **65**, 046606 (2002).

[11] W. E. Torruellas *et al.*, Phys. Rev. Lett. **74**, 5036 (1995).

[12] S. Minardi *et al.*, Opt. Lett. **26**, 1004 (2001).

[13] L. Torner and D. V. Petrov, Electron. Lett. **33**, 608 (1997); W. J. Firth and D.V. Skryabin, Phys. Rev. Lett. **79**, 2450 (1997); J. P. Torres *et al.*, J. Opt. Soc. Am. B **15**, 625 (1998).

[14] Y. V. Kartashov *et al.*, J. Opt. Soc. Am. B **19**, 2682 (2002).

[15] D. V. Petrov *et al.*, Opt. Lett. **23**, 1444 (1998).

[16] I. Towers *et al.*, Phys. Rev. E **63**, 055601(R) (2001); D. Mihalache *et al.*, Phys. Rev. Lett. **88**, 073902 (2002); Phys. Rev. E **66**, 016613 (2002).

[17] C. R. Menyuk *et al.*, J. Opt. Soc. Am. B **11**, 2434 (1994); A. V. Buryak *et al.*, Opt. Lett. **20**, 1961 (1995); O. Bang, J. Opt. Soc. Am. B **14**, 51 (1997); O. Bang *et al.*, Phys. Rev. E **58**, 5057 (1998).

[18] G. P. Agrawal, *Nonlinear Fiber Optics* (Academic Press, New York, 1995).

[19] B. A. Malomed, Phys. Rev. E **58**, 7928 (1998).

[20] Observation of transient self-narrowing of beams attributed to cubic nonlinearities in a quadratic crystal has been reported in S. Carrasco *et al.*, Opt. Lett. **27**, 2016 (2002).

[21] Ch. Bosshard *et al.*, Phys. Rev. Lett. **74**, 2816 (1995); M. J. Ablowitz *et al.*, Phys. Lett. A **236**, 520 (1997); V. V. Steblina *et al.*, J. Opt. Soc. Am. B **17**, 2026 (2000).

[22] J. P. Torres *et al.*, Opt. Lett. **27**, 1631 (2002); Opt. Commun. **213**, 351 (2002).

[23] See P. S. Julienne *et al.*, Phys. Rev. A **58**, R797 (1998); P. D. Drummond *et al.*, Phys. Rev. Lett. **81**, 3055 (1998); J. Javanainen and M. Mackie, Phys. Rev. A **59**, R3186 (1999); R. Wynar *et al.*, Science **287**, 1016 (2000); B. J. Cusack *et al.*, Phys. Rev. A **65**, 013609 (2002); E. A. Donley *et al.*, Nature (London) **417**, 529 (2002), and references therein.